PHARMACIA

Pharmacia 72: 1–13
DOI 10.3897/pharmacia.72.e149240

Research Article

Novel spirooxindole compounds as anticancer agents: targeting Plk4 kinase through design, synthesis, and molecular docking

Mervat S. Sammor[1], Almeqdad Y. Habashneh[2], Mahmoud A. Al-Sha'er[3], Sanaa K. Bardaweel[4], Mustafa M. El-Abadelah[2]

1 *Department of Basic Sciences and Humanities, Faculty of Arts and Sciences, Amman Arab University, 11953 Amman, Jordan*
2 *Faculty of Science, Chemistry Department, The University of Jordan, Amman, 11942, Jordan*
3 *Faculty of Pharmacy, Zarqa University, Zarqa, 13132, Jordan*
4 *School of Pharmacy, Department of Pharmaceutical Sciences, The University of Jordan, Amman, 11942, Jordan*

Corresponding authors: Almeqdad Y. Habashneh (a.habashneh@ju.edu.jo); Mahmoud A. Al-Sha'er (a.mahmoud@zu.edu.jo)

Received 15 February 2025 ♦ **Accepted** 15 May 2025 ♦ **Published** 13 June 2025

Citation: Sammor MS, Habashneh AY, Al-Sha'er MA, Bardaweel SK, El-Abadelah MM (2025) Novel spirooxindole compounds as anticancer agents: targeting Plk4 kinase through design, synthesis, and molecular docking. Pharmacia 72: 1–13. https://doi.org/10.3897/pharmacia.72.e149240

Abstract

Plk4 plays a crucial role in controlling the duplication of centrioles and initiating the creation of centrosomes. Disruption of Plk4 leads to aneuploidy and chromosome instability, contributing to aggressive cancers, as well as microcephaly and fatal ciliopathies in children. To effectively treat cancer, it is essential to develop potent Plk4 kinase inhibitors, which are promising anticancer agents due to their ability to induce cancer cell death and selectively target centrosome amplification. This paper examines the molecular design tools and efficient synthesis of novel spirooxindole compounds with anticancer properties, potentially mediated by Plk4 kinase suppression and consequent centrosome reduction. A potential anticancer mechanism was investigated by docking the most effective spirooxindoles into the Plk4 kinase ATPase binding site (PDB code: 4JXF, resolution: 2.40 Å). Compounds 4b and 4i showed the highest inhibition against the Caco2 and HCT116 cell lines, with IC_{50} values of 68 and 63 µM and 55 and 51 µM, respectively. Their LibDock scores were 110.12 and 109.1, suggesting that their anticancer activity may result from Plk4 enzyme inhibition. Notably, these compounds exhibited a high safety margin, with fibroblast cell line inhibition above 1000 µM. In conclusion, these findings support the potential of spirooxindole derivatives as selective and safe Plk4 inhibitors, offering a promising avenue for targeted cancer therapy with minimal toxicity to normal cells.

Graphical abstract:

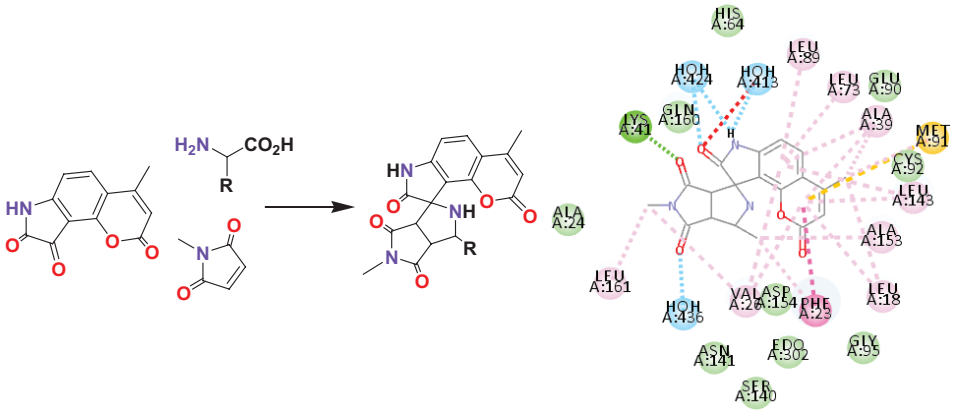

Copyright *Sammor MS et al.* This is an open access article distributed under the terms of the Creative Commons Attribution License (CC-BY 4.0), which permits unrestricted use, distribution, and reproduction in any medium, provided the original author and source are credited.

PENSOFT

Keywords

spirooxindole derivatives, docking, Plk4 inhibitors, anticancer, kinase inhibitors

Introduction

Cancer remains one of the leading causes of death worldwide and presents a major clinical challenge due to the limitations of conventional therapies such as surgery, chemotherapy, and radiation. These treatments often suffer from severe side effects, non-specific targeting, multidrug resistance, and poor therapeutic outcomes (Al-Sha'er et al. 2017; Cunningham et al. 2020; Lliaki et al. 2021; Zhang et al. 2021). Therefore, developing novel, targeted, and more effective anticancer agents is urgently needed. One promising strategy in anticancer drug discovery involves targeting key regulators of cell division. Polo-like kinase 4 (Plk4) is a serine/threonine-protein kinase that plays a central role in centrosome duplication, spindle formation, and cell cycle progression (Al-Sha'er et al. 2016, 2023). Deregulation of Plk4 leads to chromosomal instability and aneuploidy, contributing to the development of aggressive cancers. Furthermore, Plk4 dysfunction is implicated in other disorders such as microcephaly and ciliopathies (Bora et al. 2021; Yeung et al. 2022). Due to its essential role in mitotic regulation and its overexpression in various tumors, Plk4 has emerged as an attractive therapeutic target in oncology (Garvey et al. 2021; Panda et al. 2023). Recent advances in structure-based drug design have enabled the discovery of small molecules that can inhibit Plk4 activity by binding to its ATP pocket (Zhao et al. 2022). Among these, spirooxindole compounds have drawn significant interest due to their unique three-dimensional bicyclic framework and demonstrated strong anticancer potential through the inhibition of various kinases, including CDK2/5/9 and GSK-3α (Bubna 2017; Barakat et al. 2018). Naturally occurring spirocyclic oxindoles, such as mitraphylline, have shown activity against brain cancer and malignant glioma (Bacher et al. 2006; García Prado et al. 2007; García Giménez et al. 2010). Furthermore, the synthetic compound MI-888 has demonstrated potent inhibition of p53–MDM2 interactions (Zhao et al. 2013). Spiro-systems incorporating different heterocyclic moieties, such as the spirooxindole motif, have exhibited excellent potency against a broad spectrum of cancer cell lines (Yu et al. 2015; Zhou et al. 2020; Girgis et al. 2025). Similarly, the 2-(1H-indazol-6-yl)spiro[cyclopropane-1,3-indolin]-2-one derivative was identified as a potent Plk4 inhibitor, active against MDA-MB-468, MCF-7, and HCC-1954 breast cancer cells (Sampson et al. 2015). Coumarins, widely distributed in nature, also exhibit a broad range of biological activities, including anticancer effects (Zhanga and Xu 2019; Shahbaz et al. 2025). Building on this, the present study focuses on the rational design, synthesis, and biological evaluation of novel spirooxindole derivatives combined with coumarin moieties, leveraging the anticancer and pharmacological potential of both scaffolds. By combining these bioactive cores, we aimed to develop hybrid molecules with enhanced anticancer efficacy. Using a structure-guided approach, we synthesized a series of spiro[pyrano[2,3-e]indole-9,1'-pyrrolo[3,4-c]pyrrole] derivatives via a 1,3-dipolar cycloaddition reaction (Yu et al. 2015). The synthesized spirooxindole–pyrrolidine and coumarin analogues were further assessed for anticancer activity against a panel of cancer cell lines. Molecular docking studies were performed to predict the binding affinity of these compounds within the ATP-binding site of Plk4 kinase (PDB ID: 4JXF), with crystallographic water molecules retained to improve accuracy (Galliford et al. 2007). Standard anticancer agents, such as vorinostat and ellagic acid—approved by the FDA and EMA—were included for comparative *in vitro* analysis (Jossang et al. 1991; Marti and Carreira 2003).

This study investigates the therapeutic potential of newly synthesized spirooxindole–coumarin hybrids as potent Plk4 inhibitors, proposing a novel approach to selectively target cancer cell proliferation and address the limitations of existing treatments. The research was conducted through a systematic three-phase process: (1) rational design of spirooxindole derivatives aimed at the Plk4 ATP-binding site, guided by molecular docking of the proposed compounds; (2) synthesis of the top-ranked docked compounds via a 1,3-dipolar cycloaddition reaction; and (3) *in vitro* evaluation of their anticancer activity using the MTT assay.

Result and discussion

Computational docking

The Protein Data Bank file 4JXF (resolution: 2.40 Å) was selected based on its co-crystallized spiro ligand within the ATP-binding site of Plk4 kinase. To validate the docking protocol, we compared the co-crystallized pose with the redocked pose of ligand 631301, achieving an RMSD of less than 2.00 Å, indicating strong alignment and confirming the reliability of the docking procedure. The co-crystallized ligand yielded a LibDock score of 178.9, providing a benchmark for comparison with the synthesized compounds. Two-dimensional interaction analysis (Fig. 1) showed that the co-crystallized ligand interacts with the Plk4 ATP-binding site via multiple interaction modes, including direct and water-mediated hydrogen bonds, van der Waals forces, and π-interactions with hydrophobic residues. Key water-mediated hydrogen bonds were observed with HOH445, HOH419, and HOH433, contributing to binding stabilization. Additional conventional hydrogen bonds with GLU A:90, LYS A:41, CYS A:92, and GLN A:160 further anchored the ligand.

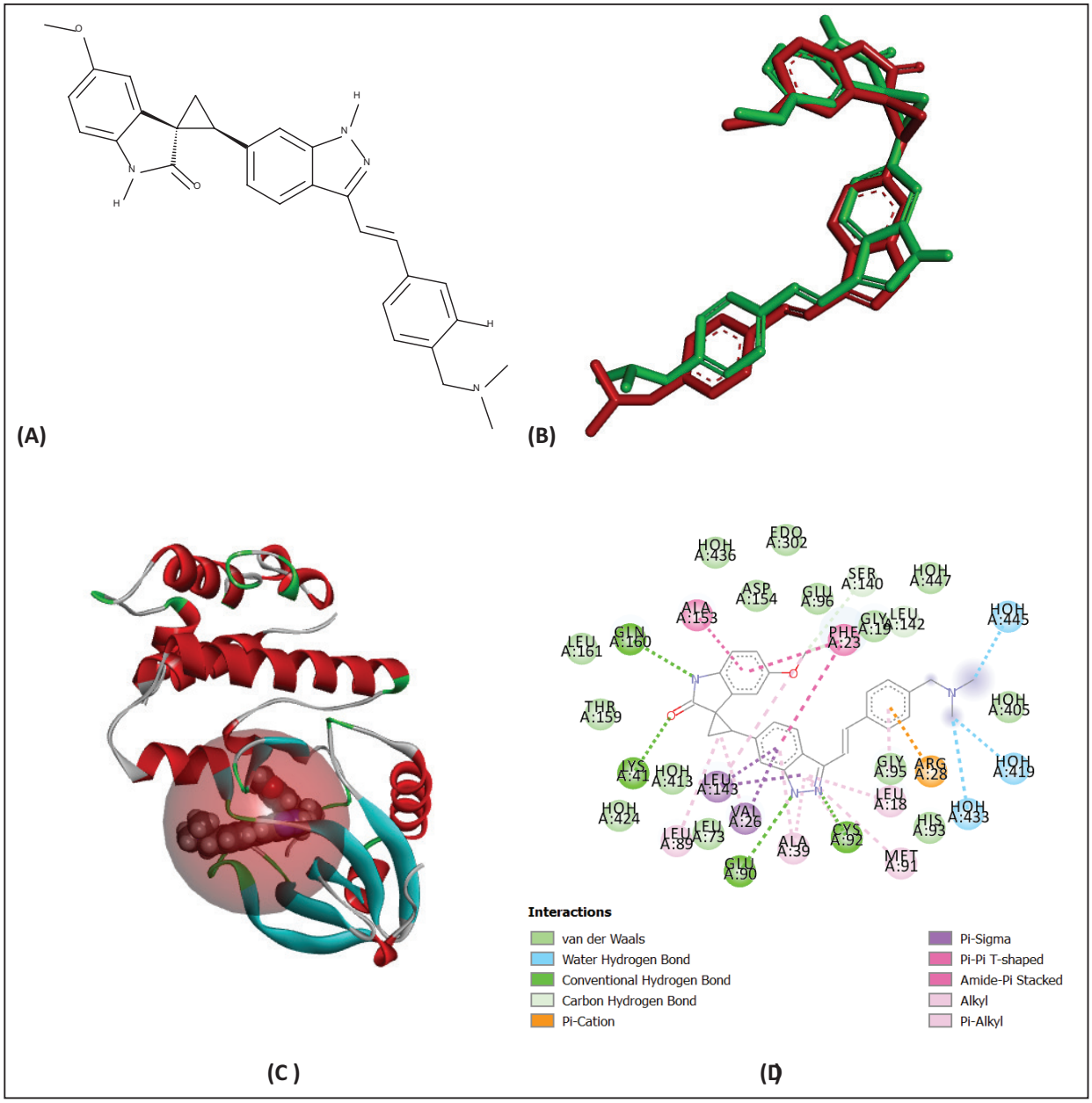

Figure 1. A. The co-crystallized spiro ligand (631301); **B.** The co-crystallized pose and the docked pose of the co-crystallized ligand (631301) with RMSD < 2.00 Å; **C.** The binding site of the Plk4 kinase protein (PDB code: 4JXF, resolution: 2.40 Å). Red represents the co-crystal compounds, and green represents the highest LibDock score compound (LibDock score = 178.9); **D.** Two-dimensional analysis of the co-crystallized ligand (631301) in the ATP binding pocket of Plk4.

The ligand also engages in π-π T-shaped and π-sigma interactions with PHE A:23 and ARG A:28, strengthening its placement within the hydrophobic environment of the ATP binding pocket. Additionally, π-alkyl stacking interactions with residues such as ALA A:153, LEU A:143, VAL A:26, and LEU A:18 contribute to ligand stability within the non-polar regions of the binding site. Alkyl interactions with hydrophobic residues like LEU A:89, LEU A:161, and LEU A:142 reinforce the binding affinity by allowing the ligand to fit tightly within the pocket. The findings suggest that synthesized compounds with similar LibDock scores and interaction profiles may exhibit favorable binding within the ATP binding site. However, like all docking studies, limitations exist, particularly regarding in vitro correlation and protein–ligand affinity prediction. Despite these challenges, the co-crystallized ligand's multi-faceted interaction profile highlights potential residues for chemical modification aimed at improving activity and specificity within the Plk4 kinase binding site. Future work may involve testing these modified compounds to enhance Plk4 kinase inhibition and assess their anti-cancer potential. Regarding Fig. 1, it can be demonstrated the following:

A. Co-crystallized spiro ligand within Plk4 protein (4JXF): The structural depiction of the co-crystallized spiro ligand highlights its unique framework, which includes functional groups likely contributing to its binding affinity within the Plk4 kinase

binding site. The spiro compound serves as a reference ligand, demonstrating how this core structure might interact with kinase proteins through various interactions, such as hydrogen bonds, van der Waals forces, and π-stacking, contributing to the overall stability of the ligand–protein complex.

B. Co-crystallized pose and docked pose of the ligand (**631301**): This comparison shows the overlay of the co-crystallized pose and the docked pose of ligand **631301**, with an RMSD of less than 2.00 Å, indicating high similarity between the two conformations. This close alignment demonstrates the accuracy of the docking model, as it can replicate the experimental binding conformation effectively. Such low RMSD values validate the docking approach and suggest that the predicted binding interactions are reliable for further analysis of ligand efficacy and stability.

C. Binding site of the Plk4 kinase protein (PDB code: 4JXF): The binding site representation of the Plk4 kinase protein highlights the key regions involved in ligand binding. Here, the co-crystal compounds are shown in red, while the compound with the highest LibDock score (178.9) is highlighted in green. The spatial overlap and interaction distribution indicate the critical residues and binding modes within the kinase's active site, with the high-scoring compound potentially showing enhanced binding interactions compared to the co-crystallized ligand.

D. Two-dimensional analysis of the co-crystallized ligand (**631301**) in the ATP binding pocket of Plk4: The two-dimensional interaction map illustrates the specific binding interactions between the co-crystallized ligand **631301** and residues within the ATP binding pocket of Plk4. Various interactions, including van der Waals forces, water-mediated hydrogen bonds, conventional hydrogen bonds, and π-stacking interactions, are displayed. These interactions highlight the ligand's multi-faceted binding strategy, ensuring strong and stable binding within the pocket. This detailed map provides insights into how ligand modifications might enhance binding affinity or selectivity by optimizing interactions with key residues.

This combined analysis underscores the effectiveness of the docking approach and the significance of specific ligand–protein interactions in drug design for Plk4 kinase inhibitors, suggesting potential modifications to improve binding affinity, activity, and anti-proliferative properties.

According to the results, the spirooxindole derivatives 4b (*R* = methyl) and 4i (*R* = *p*-hydroxybenzyl) displayed the most potent antiproliferative effects against both cancer cell lines, with IC_{50} values below 100 μM. Specifically, the IC_{50} values for the methyl-substituted derivative 4b were 68 ± 6 μM for Caco-2 and 63 ± 4 μM for HCT-116, while for the p-hydroxybenzyl-substituted derivative 4i, the values were 55 ± 3 μM for Caco-2 and 51 ± 4 μM for HCT-116. This enhanced activity may be attributed to the favorable binding interactions of the methyl and p-hydroxybenzyl side chains with the active sites of key targets within these cancer cells. Hydrophilic and hydrogen bond-forming groups in the spirooxindole derivatives 4b and 4i structures might contribute to better solubility and stronger interaction with the cancer cell membrane or intracellular proteins. Additionally, the aromatic ring of the p-hydroxybenzyl appendage in 4i could facilitate π-π stacking interactions within the cellular environment, potentially leading to more effective inhibition of proliferation pathways. Further structural and mechanistic studies could provide deeper insights into these derivatives' enhanced selectivity and efficacy.

Fig. 2 shows the 2D interaction analysis of spirooxindole derivatives 4b (*R* = methyl) and 4i (*R* = *p*-hydroxybenzyl) within the ATP binding pocket of the Plk4 enzyme, highlighting various molecular interactions. Here is a comparative discussion of each compound's interactions within the pocket:

1. Spirooxindole derivative 4b (R = methyl) interactions:

Hydrophobic interactions: Compound 4b shows van der Waals interactions with amino acids such as LEU 89, LEU 73, LEU 143, LEU 161, ALA 39, ALA 153, and VAL 26, which are common for stabilizing the ligand within the binding site.

Hydrogen bonds: Several water-mediated and conventional hydrogen bonds are evident, indicating a role in reinforcing ligand stability and positioning within the ATP pocket, such as LYS 41, HOH 413, and HOH 436.

π-interactions: π-alkyl interactions with amino acids like LEU suggest the presence of aromatic rings contributing to non-covalent stabilization. Pi-sulfur interactions with MET 91 might also contribute to this effect.

2. Spirooxindole derivative 4i (*R* = *p*-Hydroxybenzyl) interactions:

Hydrophobic Interactions: Van der Waals forces with residues like CYS 92, PHE 23, ARG 99, LEU 143, and TYR 100 anchor the ligand within the binding pocket, similar to the spirooxindole derivative 4b. Hydrogen Bonds: These derivatives form multiple water-mediated hydrogen bonds, conventional hydrogen bonds, and a carbon-hydrogen bond, contributing to robust ligand binding and orientation. π-interactions: The spirooxindole derivative 4i shows π-alkyl and π-sulfur interactions with key residues, adding to the overall stability within the ATP binding pocket, most likely due to its aromatic structure. Unique Interactions: LYS 20 and MET 91 show a π-interaction with this ligand, suggesting an additional stabilizing factor for the spirooxindole derivative 4i.

Both compounds 4b and 4i exhibit a network of interactions that help stabilize them within the ATP binding pocket of Plk4. However, the *p*-hydroxybenzyl-substituted derivative 4i demonstrates additional π-interactions, potentially making it a more stable or better-fitting ligand compared to the methyl-substitut-

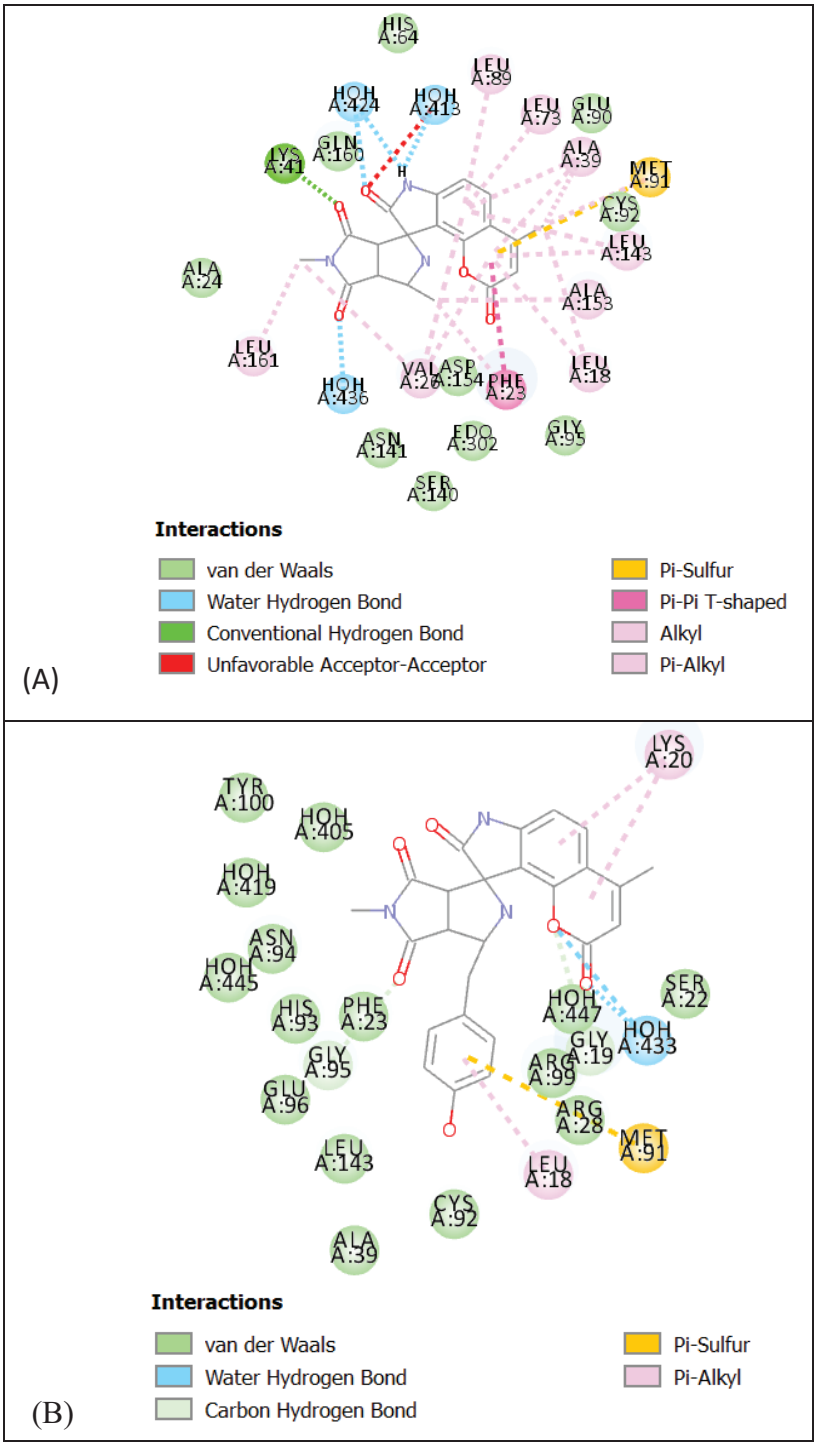

Figure 2. Two-dimensional analysis of spirooxindole derivatives 4b (*R* = methyl) and 4i (*R* = *p*-hydroxybenzyl) within the ATP binding pocket of Plk4 (PDB ID: 4JXF, resolution 2.40 Å).

ed derivative 4b. This could imply a higher binding affinity or efficacy of spirooxindole 4i in Plk4 inhibition. The spirooxindole derivative 4i binding interactions within Plk4's ATP binding site suggest a higher potential for Plk4 inhibition compared to the spirooxindole derivative 4b. This could translate to more effective cell growth inhibition in cellular assays like MTT, yielding lower cell viability results. This enhanced activity suggests that specific structural characteristics within these analogs may favorably influence their interaction with molecular targets involved in colon cancer cell survival, such as the Plk4 kinase ATP-binding site. These features likely promote stronger binding interactions, including hydrogen bonding, hydrophobic contacts, and π–π or π-alkyl stacking within the active site, as indicated by molecular docking data. In particular, the presence of electron-donating or sterically favorable groups in 4b and 4i may allow for a better spatial and electronic fit within the binding pocket, resulting in higher binding affinity and reduced IC_{50} values.

Structure–Activity Relationship (SAR)

1. Alkyl Substitution (Compound 4b): The introduction of a small hydrophobic methyl group in 4b at the R position appears to enhance antiproliferative activity. The methyl group may improve binding through hydrophobic interactions within the Plk4 binding site while maintaining molecular compactness, favoring cellular permeability.
2. Aromatic substitution with a hydroxyl group in compound 4i: The *p*-hydroxybenzyl moiety in 4i substantially improves cytotoxic potency. This enhancement may be attributed to additional hydrogen bonding or π–π stacking interactions within the Plk4 pocket, as well as increased polarity and solubility, which could facilitate better cellular uptake.
3. Bulky substituents in 4e and 4j: Compounds 4e and 4j bear a bulkier or more rigid substituent, *sec*-butyl and 3,4-dihydroxybenzyl, respectively. They achieved the highest LibDock score (129.358, 107.09); however, they showed poor *in vitro* activities. This suggests that excessive steric hindrance or suboptimal positioning within the binding pocket can reduce biological efficacy, even when predicted binding affinity is high.
4. Non-docking and inactive structures 4g and 4k: The complete lack of docking capability and activity in compounds 4g and 4k, which are attributed to phenyl and methyl-3-indolyl, respectively. These groups are possibly overly bulky, polar, or conformationally constrained. Therefore, the presence of such groups prevents proper alignment within the Plk4 active site or disrupts essential interactions, thereby abolishing activity.
5. Moderate substituents (4c, 4d, and 4f): Derivatives such as 4c, 4d, and 4f, which include medium-sized substituents (*R* = isopropyl, isobutyl, and hydroxymethyl, respectively), exhibited intermediate activity (IC_{50} between 170 and 250 μM) with relatively high docking scores (>117). These compounds 4c, 4d, and 4f may not fully exploit all key binding interactions or may suffer from reduced pharmacokinetic properties compared to 4b and 4i.

Overall, the SAR suggests that both size and functional group polarity play crucial roles in determining biological activity. Smaller hydrophobic substituents improve passive diffusion and hydrophobic interactions, while moderately polar groups with hydrogen-bonding capacity, such as hydroxylated aromatics, appear to optimize binding affinity and cytotoxicity. Conversely, overly bulky or conformationally restricted groups tend to impair activity, regardless of in silico docking performance.

Compared to the reference drug doxorubicin, which displayed potent cytotoxicity (IC_{50} = 5 ± 0.3 μM in Caco-2 and 13 ± 0.5 μM in HCT-116), the spirooxindole derivatives are moderately active. However, their high selectivity index, structural modularity, and predicted target-specific interactions underscore their potential as safer alternatives to traditional chemotherapeutics.

As shown in Table 1, compounds 4b and 4i achieved high LibDock scores (110.124 and 109.077), suggesting a strong interaction with the ATP-binding domain of Plk4 kinase. The correlation between low IC_{50} values and high docking scores supports the proposed mechanism of action and highlights these compounds as promising Plk4-targeted anticancer agents.

Table 1. The IC_{50} values (uM) of the examined compounds on 2 human colon cancer cell lines. Values are expressed as mean ± SD of three experiments with LibDock scores.

No	Caco-2	HCT-116	Fibroblasts	LibDock Score
4a	410 ± 16	421 ± 4	>1000	99.91
4b	**68 ± 6**	**63 ± 4**	**>1000**	**110.12**
4c	189 ± 11	175 ± 8	>1000	122.19
4d	180 ± 9	173 ± 7	>1000	123.59
4e	740 ± 19	756 ± 16	>1000	129.35
4f	250 ± 11	216 ± 10	>1000	117.36
4g	> 800	> 800	>1000	LibDock failed
4h	336 ± 7	312 ± 9	>1000	101.41
4i	**55 ± 3**	**51 ± 4**	**>1000**	**109.07**
4j	640 ± 19	618 ± 16	>1000	107.09
4k	> 800	> 800	>1000	LibDock failed
Doxorubicin	5 ± 0.3	13 ± 0.5	-	--

Number of trials = 3, RSD < 5%.

Future work will focus on expanding the chemical diversity at the R position, validating Plk4 inhibition through kinase assays, and evaluating pharmacokinetic properties to guide preclinical development.

Chemistry

The desired coumarin-incorporated spirooxindole compounds 4a-k were obtained via a one-pot thermal reaction of isatin 1 with the appropriate amino acid 2 in the presence of N-methylmaleimide 3 (Rehn et al. 2004; Suymka et al. 2017) (Scheme 1). The three reactants were mixed and heated under reflux in an ethanol-water (3:1) solvent system to give the desired spirooxindole compounds 4a-k in fair yields. Interestingly, in one reaction, the spirosystem and the two rings (D and E) are built on an isatin-coumarin frame structure to constitute an integral part of the five rings targeted spirooxindole compounds 4a-k.

The spirooxindole moiety was constructed through multi-steps in a one-pot reaction when the imine-carboxylic acid 5a was generated, first, *in situ* by Schiff-base reaction of the isatin 1 with the amino acid 2 (Scheme 2). Followed by the thermal decarboxylation of carboxylic acid 5a to expel CO_2 gas and generate the ylides 6 (Aly and Grigg 1988; Grigg and Sridharan 1993; Suymka et al. 2017). Eventually, the spirooxindole derivatives 4a-k were constructed via intermolecular [3+2] cycloaddition reaction of *N*-methylmaleimide 3 with azomethine ylides (1,3-dipolar species) 6. The coumarin-based isatin 1 was previously prepared as in Habashneh et al. (2012).

MS and NMR spectral data characterized the structures of the new compounds 4a-k. These data are detailed in the

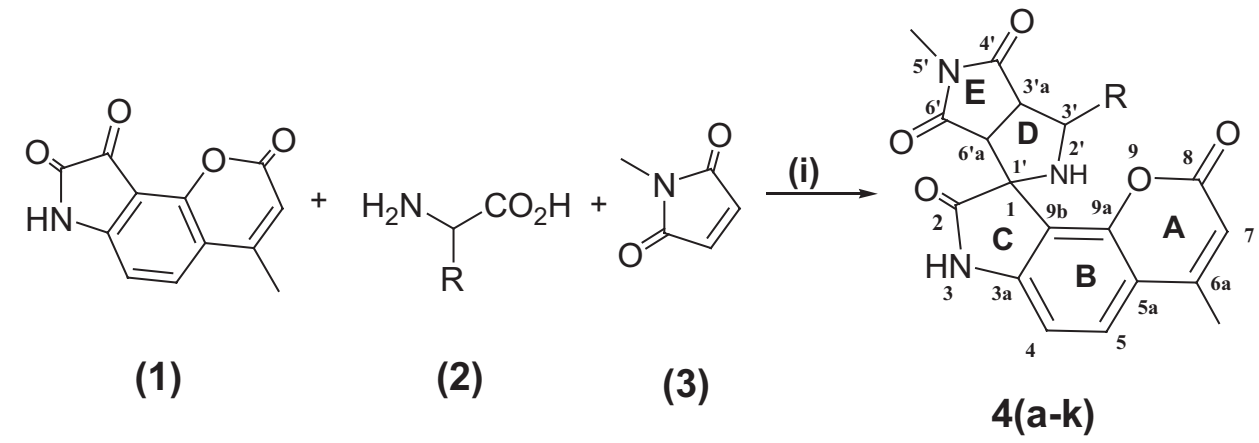

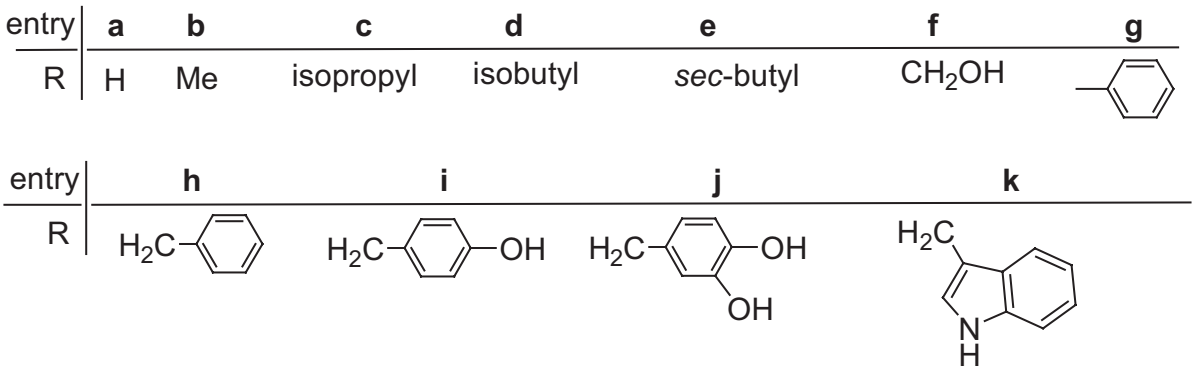

Scheme 1. Synthesis of the desired spirooxindole 4a-k.

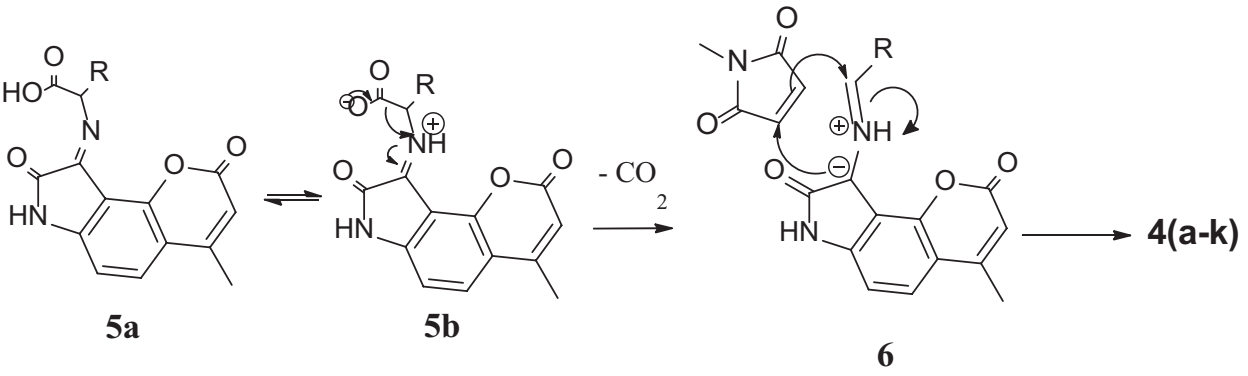

Scheme 2. The decarboxylation mechanism of the intermediate compound isatin-imino acid 5a to form ylides 6.

"Experimental Part and Supporting Information" and completely agree with the suggested structural formulas of the desired compounds 4a-k. The mass spectra display the correct molecular ion peaks, for which the measured high-resolution (HRMS-ESI) data agree with the calculated values. Furthermore, compounds approve full agreement between the experimental and theoretical isotopic patterns.

The ^{1}H and ^{13}C NMR of 4a-k confirmed the presence of the coumarin moiety (Rings A and B) incorporated in the structures of these compounds; All ^{1}H NMR spectra revealed a singlet peak at 2.37 ppm related to the methyl at C-6, a singlet peak at 6.15 ppm related to the proton at C-7; and both protons at C-4 and C-5 appeared as two doublet peaks at 6.67 and 7.88 ppm, respectively. On the other hand, ^{1}H NMR spectra of the desired compounds 4a-k confirmed the presence of the newly introduced *N*-methyltetrahydropyrrolopyrrole-1,3-dione bicyclic moiety (Rings D and E); the methyl group at N5' resonated as a singlet at 2.85 ppm, and the N2'-H proton appeared as a singlet at 3.51 ppm. Furthermore, the two protons at the two bridging carbon atoms, C3'a and 6'a, resonated as triplets and doublets at 3.59 and 3.43 ppm, respectively. The N3–H proton in the pyrrolidinone cycle (Ring C) resonated as a singlet at 10.90 ppm. All ^{13}C NMR

spectra of spirooxindole compounds 4a–k showed the spirocarbon (C1,1′) at about 69.8 ppm (Rehn et al. 2004). Eventually, the ^{1}H and ^{13}C NMR spectra of 4a-k revealed only one set of peaks, which strongly indicated that these compounds are formed as single diastereoisomers during the 1,3-cycloaddition reactions occurring in a concerted, stereo-controlled manner.

In vitro analysis

The antiproliferative effects of the synthesized compounds were assessed using the MTT assay, with IC_{50} values determined against two human colon cancer cell lines, Caco-2 and HCT-116, as summarized in Table 1. All tested compounds demonstrated a favorable safety profile, exhibiting IC_{50} values exceeding 1000 μM in normal fibroblast cells, thereby indicating selective cytotoxicity toward cancerous cells. Among the evaluated derivatives, spirooxindole analogs 4b (*R* = methyl) and 4i (*R* = *p*-hydroxybenzyl) showed the most potent anticancer activity, with IC_{50} values below 100 μM in both cancer cell lines. Specifically, compound 4b displayed IC_{50} values of 68 ± 6 μM (Caco-2) and 63 ± 4 μM (HCT-116), while 4i exhibited enhanced potency with IC_{50} values of 55 ± 3 μM and 51 ± 4 μM, respectively. These results are consistent with molecular interaction data, suggesting that the improved antiproliferative activity of compound 4i may stem from its favorable binding characteristics within the Plk4 kinase ATP-binding domain. The MTT assay outcomes support this mechanistic hypothesis, as lower IC_{50} values correlate with stronger binding interactions predicted through molecular modeling. Overall, the structural features of 4b and 4i appear to contribute significantly to their biological efficacy, warranting further investigation into their therapeutic potential.

Conclusion

In this study, novel spirooxindole-coumarin hybrid derivatives were synthesized and evaluated for their potential as Plk4 kinase inhibitors in cancer therapy. Among the tested compounds, the p-hydroxybenzyl-substituted compound 4i exhibited the greatest potency against Caco-2 and HCT-116 colon cancer cell lines, with IC_{50} values of 55 μM and 51 μM, respectively, while maintaining high selectivity and safety, as evidenced by IC_{50} values exceeding 1000 μM in normal fibroblast cells. Less antiproliferative activity was demonstrated by compound 4b (methyl-substituted) in the same cell lines, with IC_{50} values of 68 μM and 63 μM. The activity of compound 4i is attributed to its enhanced binding interactions within the Plk4 ATP-binding site, supported by a higher LibDock score and a rich network of stabilizing molecular contacts. These findings position spirooxindole derivative 4i as a lead compound for further preclinical development as a selective Plk4-targeting anticancer agent.

Experimental

Computational docking

Computational docking is a widely used in silico technique that predicts stable interactions between a small molecule and a larger biological receptor (Cui et al. 1996). It effectively simulates the binding of chemical and biological targets, providing insights into molecular recognition and interaction patterns (Cui et al. 1996). LibDock, a structure-based docking tool, utilizes the geometry of protein binding sites to perform docking simulations (Edmondon et al. 1999). It generates multiple ligand conformations, identifies polar and apolar interaction hot spots, aligns these with the binding pocket, and subsequently optimizes and scores the ligand poses (García et al. 2010). The success of docking in distinguishing active compounds from inactive ones (decoys) largely depends on the structural similarity between screened ligands and the co-crystallized ligand used in the docking protocol (Al-Sha'er et al. 2016; Al-Sha'er et al. 2017; Al-Sha'er et al. 2023). Based on these criteria, we selected the Plk4 kinase protein structure (PDB ID: 4JXF, resolution: 2.40 Å), which includes a co-crystallized spiro ligand (631301), as the docking template for our study. The 3D structure of Plk4 (PDB ID: 4JXF) was obtained from the Protein Data Bank (PDB), and Gasteiger–Marsili charges were assigned to the protein atoms using the DS 4.5 FER module. The protein wasused directly in the docking studies without energy minimization. Explicit water molecules were retained as required by the docking protocol, which involved docking in the presence of water.

Docking protocol (LibDock settings):

LibDock, a site-feature-based docking algorithm, was employed to dock ligands—after removal of hydrogen atoms—into the active site guided by binding hotspots. This method considers ligand flexibility while treating the receptor as rigid. The docking workflow involved the following settings:

1. Ligand conformations were generated using the Discovery Studio CAT-CONFIRM module, allowing up to 250 conformers per ligand within an energy threshold of 20 kcal/mol from the most stable conformer, utilizing the fast conformer generation option.
2. A binding site sphere with a radius of 12.10 Å was defined around the center of the co-crystallized ligand (**631301**).
3. The number of binding site hotspots was set to a maximum of 100.
4. The RMSD tolerance for ligand-to-hotspot matching was set to 0.25 Å.
5. Up to 100 poses per ligand were saved during the hotspot matching step before final pose minimization.
6. A maximum of 100 final poses per ligand were retained within the binding pocket.
7. A minimum LibDock score of 100 was set as the threshold; poses below this score were excluded.

8. The final pose optimization used a maximum of 50 rigid body minimization steps via the BFGS method.
9. Pose-hotspot alignment was terminated if steric clashes exceeded 10% of the ligand's heavy atom count.
10. Successful poses were required to have a nonpolar solvent-accessible surface area ≤ 15.0 Å².
11. Successful poses were also required to have a polar solvent-accessible surface area ≤ 5.0 Å².
12. No final minimization of the ligand within the binding pocket was performed.

Chemistry

All syntheses were carried out under aerobic conditions. All chemicals, including solvents, were purchased from suppliers and used without additional purification. 7-Amino-4-methylcoumarin was synthesized following procedures described in the literature (Pozdnev 1990). Melting points were determined on a Stuart Scientific melting point apparatus in open capillary tubes. ^{1}H and ^{13}C NMR spectra were recorded on a 500 MHz spectrometer (Bruker AVANCE-III). Chemical shifts are expressed in δ units; ^{1}H–^{1}H coupling constants are given in Hertz. High-resolution mass spectra (HRMS) were acquired by the electrospray ionization (ESI) technique using a Bruker APEX-2 instrument. The samples were dissolved in acetonitrile, diluted in spray solution (methanol/water 1:1 v/v with 0.1% formic acid), and infused using a syringe pump at a flow rate of 2 mL/min. External calibration was conducted using an arginine cluster in the mass range m/z 175–871.

General procedure for the three-component reaction yielding the spiro-oxindoles 4a-k:

The amino acid 2a–2j (1.1 mmol) and N-methylmaleimide 3 (1.0 mmol) were added to a suspension of isatin 1 (1.0 mmol) in 12 cm^3 of solvent (9 cm^3 methanol: 3 cm^3 water). The reaction mixture was heated under reflux at 90 °C for 18 hr. During heating under reflux, CO_2 was expelled, and a clear solution was obtained. The reaction mixture was quenched by pouring it into a mixture of saturated aqueous $NaHCO_3$ (150 cm3) with ice. The solid crude product was collected by suction filtration, washed with water, and dried. Then, pure solid products were obtained by recrystallization from ethanol.

4,5'-dimethyl-3',3a'-dihydro-2H,2'H-spiro[pyrano[2,3-e]indole-9,1'-pyrrolo[3,4-c]pyrrole]-2,4',6',8(5'H,6a'H,7H)-tetraone (4a)

The amino acid that was used to prepare 4a is glycine 2a. Yield = 43.4%, mp 335 °C, ^{1}H NMR (500 MHz, DMSO-d$_6$): d 2.37 (s, 3H, C6-C*H*$_3$), 2.85 (s, 3H, NCH$_3$), 3.43 (d, *J* 9.9 Hz, 1H, H-6'a), 3.59 (pseudo-t, *J* 7.8 Hz, 1H, H-3'a), 3.77 (m, 1H, H-3'), 3.51 (br s, H–N(2'), exchangeable with D$_2$O), 6.15 (s, 1H, H-7), 6.87 (d, *J* 8.1 Hz, 1H, H-4), 7.68 (d, *J* 8.2 Hz, 1H, H-5), 10.88 (s, 1H, H–N(3), exchangeable with D$_2$O) ppm; ^{13}C NMR (125 MHz, DMSO-d$_6$): d 18.8 (C6-*C*H$_3$), 25.4 (NCH$_3$), 47.7 (C-3'a), 47.8 (C-3'), 51.9 (C-6'a), 69.8 (spiro C-1,1'), 107.4 (C-4), 111.6 (C-7), 112.0 (C-5a), 115.7 (C-9b), 128.4 (C-5), 146.8 (C-3a), 151.2 (C-9a), 154.4 (C-6), 159.8 (C-8), 176.2 (C-6'), 179.5 (C-4'),180.3 (C-2), HRMS (ESI) m/z: [M+H]$^+$ calcd for $C_{18}H_{16}N_3O_5$, 354.10845; found 354.10595.

3',4,5'-trimethyl-3',3a'-dihydro-2H,2'H-spiro[pyrano[2,3-e]indole-9,1'-pyrrolo[3,4-c]pyrrole]-2,4',6',8(5'H,6a'H,7H)-tetraone (4b)

The amino acid that was used to prepare 4b is alanine 2b. Yield = 32.4%, mp 296 °C, ^{1}H NMR (500 MHz, DMSO-d$_6$): d 1.23 (d, *J* 6.0 Hz, 3H, CHC*H*$_3$), 2.37 (s, 3H, C6-C*H*$_3$), 2.83 (s, 3H, NCH$_3$), 3.41 (d, *J* 7.7 Hz, 1H, H-6'a), 3.44 (pseudo-t, *J* 8.3 Hz, 1H, H-3'a), 4.30 (m, 1H, H-3'), 4.20 (br s, 1H, H–N(2'), exchangeable with D$_2$O), 6.15 (s, 1H, H-7), 6.86 (d, *J* 8.1 Hz, 1H, H-4), 7.68 (d, *J* 8.1 Hz, 1H, H-5), 10.86 (br s, 1H, H–N(3), exchangeable with D$_2$O). ^{13}C NMR (125 MHz, DMSO-d$_6$): d 17.3 (CH*C*H$_3$), 18.8 (C6-*C*H$_3$), 25.1 (NCH$_3$), 49.4 (C-3'a), 52.2 (C-6'a), 53.4 (C-3'), 69.1 (spiro C-1,1'), 107.3 (C-4), 111.6 (C-7), 112.7 (C-9b), 115.0 (C-5a), 128.4 (C-5), 146.6 (C-3a), 151.4 (C-9a), 154.3 (C-6), 159.5 (C-8), 176.1 (C-6'), 179.8 (C-4'),180.7 (C-2), HRMS ((+)-ESI), m/z: [M + H]$^+$ calcd for $C_{19}H_{18}N_3O_5$, 368.12410; found 368.12163.

3'-isopropyl-4,5'-dimethyl-3',3a'-dihydro-2H,2'H-spiro[pyrano[2,3-e]indole-9,1'-pyrrolo[3,4-c]pyrrole]-2,4',6',8(5'H,6a'H,7H)-tetraone (4c)

The amino acid that was used to prepare 4c is valine 2c. Yield = 57.2%, mp > 390 °C, ^{1}H NMR (500 MHz, DMSO-d$_6$): d 0.87 (d, *J* 6.3 Hz, 3H, CH(C*H*$_3$)$_2$), 1.15 (d, *J* 5.9 Hz, 3H, CH(C*H*$_3$)$_2$), 1.89 (m, 1H, C*H*(Me)$_2$), 2.37 (s, 3H, C6-C*H*$_3$), 2.81 (s, 3H, NCH$_3$), 3.52 (d, *J* 5.6 Hz, 1H, H-6'a), 3.54 (pseudo-t, *J* 8.4 Hz, 1H, H-3'a), 3.84 (m, 1H, H-3'), 4.35 (br s,1H, H–N(2'), exchangeable with D$_2$O), 6.15 (s, 1H, H-7), 6.85 (d, *J* 8.2 Hz, 1H, H-4), 7.67 (d, *J* 8.2 Hz, 1H, H-5), 10.83 (br s, 1H, H–N(3), exchangeable with D$_2$O). ^{13}C NMR (125 MHz, DMSO-d$_6$): d 19.0 (C6-*C*H$_3$), 21.7, 21.8(CH(*C*H$_3$)$_2$), 25.4 (NCH$_3$), 29.9 (C*H*(Me)$_2$), 48.0 (C-3'a), 52.1 (C-6'a), 65.6 (C-3'), 68.6(spiroC-1,1'), 107.3 (C-4), 111.6 (C-7), 113.1 (C-5a), 115.0 (C-9b), 128.3 (C-5), 146.8 (C-3a), 151.4 (C-9a), 154.3 (C-6), 159.7 (C-8), 175.9 (C-6'), 177.0 (C-4'), 180.9 (C-2) ppm; HRMS ((+)-ESI): m/z; [M + Na]$^+$calcd. for $C_{21}H_{21}N_3NaO_5$, 418.13734; found 418.13739.

3'-isobutyl-4,5'-dimethyl-3',3a'-dihydro-2H,2'H-spiro[pyrano[2,3-e]indole-9,1'-pyrrolo[3,4-c]pyrrole]-2,4',6',8(5'H,6a'H,7H)-tetraone (4d)

The amino acid that was used to prepare 4d is leucine 2d. Yield = 23.6%, mp 181–183 °C, ^{1}H NMR (500 MHz, DMSO-d$_6$): d 0.90 (d, *J* 6.2 Hz, 6H, CH(C*H*$_3$)$_2$), 1.31, 1.69 (m, 2H, C*H*$_2$CHMe$_2$), 1.79 (m, 1H, C*H*Me$_2$), 2.37 (s, 3H, C6-C*H*$_3$), 2.82 (s, 3H, NCH$_3$), 3.38 (d, *J* 6.6 Hz, 1H, H-6'a),

3.45 (pseudo-t, *J* 7.6 Hz, 1H, H-3'a), 4.28 (m, 1H, H-3'), 4.20 (br s,1H, H–N(2'), exchangeable with D_2O), 6.15 (s, 1H, H-7), 6.86 (d, *J* 8.2 Hz, 1H, H-4), 7.68 (d, *J* 8.1 Hz, 1H, H-5), 10.88 (br s, 1H, H–N(3), exchangeable with D_2O). ^{13}C NMR (125 MHz, DMSO-d_6): d 19.0 (C6-*C*H_3), 22.9, 23.9(CH(*C*H_3)$_2$), 25.4 (NCH_3), 26.0 (*C*HMe_2), 40.8 (*C*H$_2$CHMe_2), 49.0 (C-3'a), 52.2 (C-6'a), 56.4 (C-3'), 68.9 (spiro C-1,1'), 107.3 (C-4), 111.6 (C-7), 112.8 (C-5a), 115.0 (C-9b), 128.4 (C-5), 146.8 (C-3a), 151.3 (C-9a), 154.3(C-6), 159.6 (C-8), 176.0 (C-6'), 177.0 (C-4'), 180.7 (C-2). HRMS ((+)-ESI): m/z; $[M + H]^+$ calcd. for $C_{22}H_{24}N_3O_5$, 410.17105; found 410.17077.

3'-(sec-butyl)-4,5'-dimethyl-3',3a'-dihydro-2H,2'H-spiro[pyrano[2,3-e]indole-9,1'-pyrrolo[3,4-c]pyrrole]-2,4',6',8(5'H,6a'H,7H)-tetraone (4e)

The amino acid that was used to prepare 4e is isoleucine 2e. Yield = 37.5%, mp 239 °C, ^1H NMR (500 MHz, DMSO-d_6): d 0.93 (pseudo-t, *J* 7.1 Hz, 3H, CH$_2$C*H*$_3$), 1.50 (m, 2H, C*H*$_2$Me), 1.13 (d, *J* 6.2 Hz, 3H, CHC*H*$_3$), 1.93 (m, 1H, C*H*Me), 2.37 (s, 3H, C6-C*H*$_3$), 2.81 (s, 3H, NCH_3), 3.47 (d, *J* 5.5 Hz, 1H, H-6'a), 3.54 (pseudo-t, *J* 7.5 Hz, 1H, H-3'a), 3.94 (m, 1H, H-3'), 4.19 (br s, 1H, H–N(2'), exchangeable with D_2O), 6.14 (s, 1H, H-7), 6.85 (d, *J* 8.2 Hz, 1H, H-4), 7.67 (d, *J* 8.0 Hz, 1H, H-5), 10.83 (br s, 1H, H–N(3), exchangeable with D_2O). ^{13}C NMR (125 MHz, DMSO-d_6): d 11.8 (CH2*C*H$_3$), 17.5 (CH*C*H$_3$), 19.0 (C6-*C*H$_3$), 25.4 (NCH_3), 27.7 (CH*C*H$_2$), 36.1 (*C*HCH$_2$Me), 48.2 (C-3'a), 52.1 (C-6'a), 64.1 (C-3'), 68.7 (spiro C-1,1'), 107.3 (C-4), 111.6 (C-7), 113.1 (C-5a), 115.0 (C-9b), 128.3 (C-5), 146.8 (C-3a), 151.4 (C-9a), 154.3(C-6), 159.7 (C-8), 175.9 (C-6'), 177.0 (C-4'), 180.9 (C-2) ppm; HRMS ((+)-ESI): m/z; $[M + H]^+$ calcd. for $C_{22}H_{24}N_3O_5$, 410.17105; found 410.17042 .

3'-(hydroxymethyl)-4,5'-dimethyl-3',3a'-dihydro-2H,2'H-spiro[pyrano[2,3-e]indole-9,1'-pyrrolo[3,4-c]pyrrole]-2,4',6',8(5'H,6a'H,7H)-tetraone (4f)

The amino acid that was used to prepare 4f is serine 2f. Yield = 72.6%, mp 317 °C, ^1H NMR (500 MHz, DMSO-d_6): d 2.37 (s, 3H, C6-C*H*$_3$), 2.82 (s, 3H, NCH_3), 3.45, 3.88 (m, 2H, C*H*$_2$OH), 3.50 (pseudo-t, *J* 8.0 Hz, 1H, H-3'a), 3.64 (d, *J* 5.1 Hz, 1H, H-6'a), 4.27 (m, 1H, H-3'), 4.58 (s, 1H, CH2O*H*, exchangeable with D_2O), 4.35 (br s, 1H, H–N(2'), exchangeable with D_2O), 6.14 (s, 1H, H-7), 6.85 (d, *J* 8.2 Hz, 1H, H-4), 7.67 (d, *J* 8.2 Hz, 1H, H-5), 10.83 (br s, 1H, H–N(3), exchangeable with D_2O). ^{13}C NMR (125 MHz, DMSO-d_6): d 19.0 (C6-*C*H_3), 25.4 (NCH_3), 47.4 (C-3'a), 51.9 (C-6'a), 59.9 (C-3'), 62.4 (CH*C*H$_2$), 68.9 (spiro C-1,1'), 107.1 (C-4), 111.4 (C-7), 112.8 (C-5a), 115.0 (C-9b), 128.1 (C-5), 146.8 (C-3a), 151.4 (C-9a), 154.3 (C-6), 159.6 (C-8), 176.0 (C-6'), 177.0 (C-4'),180.9 (C-2) ppm; HRMS (ESI) m/z; $[M - H]^-$ calcd. for $C_{19}H_{16}N_3O_6$, 382.10336; found 382.10260.

4,5'-dimethyl-3'-phenyl-3',3a'-dihydro-2H,2'H-spiro[pyrano[2,3-e]indole-9,1'-pyrrolo[3,4-c]pyrrole]-2,4',6',8(5'H,6a'H,7H)-tetraone (4g)

The amino acid which was used to prepare 4g is phenylglycine, 2g. Yield = 63.8%, mp 307 °C, ^1H NMR (500 MHz, DMSO-d_6): d 2.40 (s, 3H, C6-C*H*$_3$), 2.74 (s, 3H, NCH_3), 3.42 (d, *J* 7.9 Hz, 1H, H-6'a), 3.72 (pseudo-t, *J* 8.0 Hz,1H, H-3'a), 4.05 (br s, 1H, H–N(2'), exchangeable with D2O), 5.42 (pseudo-t, *J* 4.0, 1H, H-3'), 6.19 (s, 1H, H-7), 6.88 (d, *J* 8.2 Hz, 1H, H-4), 7.25 (m, 3H, H-4", H-3"/H-5"), 7.42 (d, *J* 7.4Hz, 2H, H-2"/H-6"), 7.70 (d, *J* 8.2 Hz, 1H, H-5), 10.86 (br s, 1H, H–N(3), exchangeable with D_2O); ^{13}C NMR (125 MHz, DMSO-d_6): d 18.9 (C6-*C*H_3), 25.1(NCH_3), 50.4 (C-3'a),51.3 (C-6'a), 61.4(C-3'), 68.7 (spiro C-1,10), 107.3 (C-4), 111.5 (C-7), 113.3 (C-5a), 115.1 (C-9b), 127.6 (C-4"), 128.0 (C-5, C-2"/C-6"), 128.2 (C-3"/C-5"), 140.1 (C-1"), 146.7 (C-3a), 151.6 (C-9a), 154.3 (C-6), 159.7 (C-8), 175.7 (C-4', C-6'), 181.5 (C-2) ppm HRMS (ESI) m/z; $[M + H]^+$ calcd. for $C_{24}H_{20}N_3O_5$, 430.13975; found 430.13964.

3'-benzyl-4,5'-dimethyl-3',3a'-dihydro-2H,2'H-spiro[pyrano[2,3-e]indole-9,1'-pyrrolo[3,4-c]pyrrole]-2,4',6',8(5'H,6a'H,7H)-tetraone (4h)

The amino acid used to prepare for 4 hours is phenylalanine. Yield = 79.1%,mp 311 °C, ^1H NMR (500 MHz, DMSO-d_6): d 2.37 (s, 3H, C6-C*H3*), 2.60 (m, 2H, C*H*$_2$Ph), 2.86 (s, 3H, NCH_3), 3.52 (d, *J* 9.1Hz, 1H, H-6'a), 4.38 (pseudo-t, *J* 5.1 Hz, 1H, H-3'a), 4.43 (m, 1H, H-3'), 4.38 (br s, 1H, H–N(2'), exchangeable with D_2O), 6.17 (s, 1H, H-7), 6.83 (d, *J* 8.3 Hz, 1H, H-4), 7.18 (pseudo-t, *J* 6.3 Hz, 1H, H-4"), 7.26 (pseudo-t, J = 6.8 Hz, 2H, H-3"/H-5"), 7.32 (d, 2H, H-2"/H-6"), 7.67 (d, *J* 8.0 Hz, 1H, H-5), 10.81(br s, 1H, H–N(3), exchangeable with D_2O); ^{13}C NMR (125 MHz, DMSO-d_6): δ = 18.9 (C6-*C*H_3), 25.3 (NCH_3), 37.5 (*C*H$_2$Ph), 48.6 (C-3'a), 51.9 (C-6'a), 59.7 (C-3'), 68.7 (spiro C-1,10), 107.1 (C-4), 111.4 (C-7), 112.7 (C-5a), 115.0 (C-9b), 126.4 (C-4"), 128.1 (C-5), 128.6 (C-2", C-6"), 129.4 (C-3", C-5"), 140.5 (C-1"), 146.8 (C-3a), 151.4 (C-9a), 154.3 (C-6), 159.6 (C-8), 175.9 (C-6'), 177.1 (C-4'), 180.8 (C-2) ppm; HRMS (ESI) m/z; $[M + H]^+$ calcd. for $C_{25}H_{22}N_3O_5$, 444.15540; found 444.15529.

3'-(4-hydroxy benzyl)-4,5'-dimethyl-3',3a'-dihydro-2H,2'H-spiro[pyrano[2,3-e]indole-9,1'-pyrrolo[3,4-c]pyrrole]-2,4',6',8(5'H,6a'H,7H)-tetraone (4i)

The amino acid that was used to prepare 4i is tyrosine 2i. Yield = 25.7%, mp > 390 °C, ^1H NMR (500 MHz, DMSO-d_6): d 2.37 (s, 3H, C6-C*H*$_3$), 2.38 (dd, *J* 10.5 Hz, 17.4 Hz, 1H, benzylic C*H*$_2$), 2.85 (s, 3H, NCH_3), 3.20 (dd, *J* 4.8 Hz, 13.9 Hz, 1H, C*H*$_2$Ph), 3.49 (d, *J* 7.3 Hz, 1H, H-6'a), 3.67 (pseudo-t, *J* 7.6 Hz, 1H, H-3'a), 4.35 (m, 1H, H-3'), 4.21 (br s, 1H, H–N(2'), exchangeable with D_2O), 6.16 (s, 1H, 7-H), 6.64 (d, *J* 7.9 Hz, 2H, H-3", H-5"), 7.09 (d, *J* 7.9 Hz, 2H, H-2", H-6"), 7.55 (d, *J* 8.2 Hz, 1H, H-4), 7.96 (d, *J* 8.2 Hz, 1H, H-5), 9.15 (s, 1H, PhOH, exchangeable with

D_2O), 10.81 (br s, 1H, H–N(3), exchangeable with D_2O). ^{13}C NMR (125 MHz, DMSO-d_6): d 19.0 (C6-*C*H_3), 25.4 (NCH_3), 36.9 (*C*H_2Ph), 48.7 (C-3'a), 52.1 (C-6'a), 60.3 (C-3'), 68.7(spiro C-1,1'), 107.3 (C-4), 111.6 (C-7), 112.8 (C-5a), 115.0 (C-9b), 115.6 (C-3"/C-5"), 128.3 (C-5), 130.4 (C-2"/ C-6"), 130.6 (C-1"), 146.8 (C-3a), 151.4 (C-9a), 154.3 (C-6),156.0 (C-4"), 159.8 (C-8), 176.0 (C-6'),177.1 (C-4'), 180.8 (C-2); HRMS (ESI) m/z; $[M+H]^+$ calcd. for $C_{25}H_{22}N_3O_6$, 460.15031; found 460.15010.

3'-(3,4-dihydroxybenzyl)-4,5'-dimethyl-3',3a'-dihydro-2H,2'H-spiro[pyrano[2,3-e]indole-9,1'-pyrrolo[3,4-c]pyrrole]-2,4',6',8(5'H,6a'H,7H)-tetraone (4j)

The amino acid that was used to prepare 4j is doad 2j. Yield = 22.9%, mp > 390 °C, ^1H NMR (500 MHz, DMSO-d_6): d 2.37 (s, 3H, C6-C*H*$_3$), 2.38 (dd, *J* 10.5 Hz, 17.4 Hz, 1H, benzylic C*H*$_2$), 2.85 (s, 3H, NCH_3), 3.14 (dd, *J* 5.2 Hz, 14.2 Hz,1H, benzylic C*H*$_2$), 3.42 (d, *J* 5.8 Hz, 1H, H-6'a), 3.47 (pseudo-t, *J* 7.6 Hz, 1H, H-3'a), 4.35 (m, 1H, H-3'), 4.20 (br s, 1H, H–N(2'), exchangeable with D_2O), 6.16 (s, 1H, H-7), 6.53 (d, *J* 8.9Hz, 1H, H-6"), 6.60 (d, *J* 8.4Hz, 1H, H-5"), 6.70 (s, 1H, H-2"), 6.82 (d, *J* 8.2 Hz, 1H, H-4), 7.66 (d, *J* 8.2Hz, 1H, H-5), 8.56, 8.71, (s, 2H, (OH)2), 10.79 (br s, 1H, H–N(3), exchangeable with D_2O) ppm; ^{13}C NMR (125 MHz, DMSO-d_6): d 19.0 (C6-*C*H_3), 25.4 (NCH_3), 37.1 (*C*H_2Ph), 48.7 (C-3'a), 52.1 (C-6'a), 60.2 (C-3'), 68.7(spiro C-1,1'), 107.1 (C-4), 111.6 (C-7), 113.0 (C-5a), 115.0 (C-9b), 116.0 (C-5"), 117.0 (C-2"), 120.2 (C-6"), 128.3 (C-5), 131.3 (C-1"), 143.9 (C-3a), 145.3 (C-4"), 146.8 (C-3"), 151.3 (C-9a), 154.4 (C-6),159.7 (C-8), 176.0 (C-6'),177.1 (C-4'), 180.8 (C-2); HRMS (ESI) m/z; $[M - H]^-$ calcd. For $C_{25}H_{20}N_3O_7$, 474.13067; found 475.12637

3'-((1H-indol-3-yl)methyl)-4,5'-dimethyl-3',3a'-dihydro-2H,2'H-spiro[pyrano[2,3-e]indole-9,1'-pyrrolo[3,4-c]pyrrole]-2,4',6',8(5'H,6a'H,7H)-tetraone (4k)

The amino acid that was used to prepare 4k is tryptophan 2k. Yield = 76.6%, mp 300 °C; ^1H NMR (500 MHz, DMSO-d_6): d 2.37 (s, 3H, C6-C*H*$_3$), 2.76 (dd, *J* 14.4, 7.9 Hz, 2H, C*H*$_2$-indole), 2.88 (s, 3H, NCH_3), 3.46 (d, *J* 5.2 Hz, 1H, H-6'a), 3.56 (pseudo-t, *J* 7.5 Hz, 1H, H-3'a), 4.56 (m, 1H, H-3'), 4.37(br s, 1H, H–N(2'), exchangeable with D_2O), 6.17 (s, 1H, H-7), 6.83 (d, *J* 8.2 Hz, 1H, H-4), 6.95 (pseudo-t, *J* 7.2Hz, 1H, H-5"), 7.04 (pseudo-t, J = 7.4 Hz, 1H, H-6"), 7.22 (d, J = 7.7 Hz, 1H, H-2"),7.32 (d, J = 7.9Hz,1H, H-4"), 7.54 (d, *J* 7.7Hz, 1H, H-7"), 7.66 (d, *J* 8.2 Hz, 1H, H-5), 10.78(br s, 2H, H–N(3), H–N(3"), exchangeable with D_2O). ^{13}C NMR (125 MHz, DMSO-d_6): d 19.1 (C6-*C*H_3), 25.4 (NCH_3), 27.5 (*C*H_2-indole), 48.7 (C-3'a), 52.2 (C-6'a), 59.0 (C-3'), 68.8 (spiro C-1,1'), 107.3 (C-4), 111.6(C-4"), 111.9 (C-7), 112.6 (C-5a), 112.9 (C-1"), 115.0 (C-9b), 118.8 (C-7"), 118.9 (C-6"), , 121.4 (C-5"), 123.9 (C-2"), 127.8 (C-7a"), 128.3 (C-5), 136.6 (C-3a"), 146.8 (C-3a), 151.4 (C-9a), 154.3 (C-6),159.7 (C-8), 176.0 (C-6'),177.1 (C-4'), 180.8 (C-2) HRMS (ESI) m/z; $[M - H]^-$ calcd. for $C_{27}H_{21}N_4O_5$, 481.15174; found 481.14665.

Antiproliferative activity

The cell lines were procured from the American Type Culture Collection (ATCC, Rockville, MD, USA). Cells were maintained in Dulbecco's Modified Eagle Medium (DMEM) (Invitrogen, USA), supplemented with 10% heat-inactivated fetal bovine serum (HI-FBS) (Invitrogen), 2 mmol L^{-1} of L-glutamine, 50 U mL^{-1} of penicillin, and 50 µg mL^{-1} of streptomycin. Cultures were maintained in a controlled environment with 5% CO_2 and 95% relative humidity at 37 °C. All cells were plated at a density of $8 \times 10^{\wedge 3}$ cells per well in 96-well plates and incubated for 24 hours to allow adhesion. The compounds under investigation were dissolved in DMSO and diluted in culture media to achieve the required concentrations. Each concentration was tested in three triplicates, and this was repeated in three independent assays, resulting in a total of 9 triplicate assays for each compound.

Test samples were incubated for 24 hours at 37 °C in a 5% CO_2 incubator. Following the incubation period, an MTT assay was performed as previously described (Bardaweel et al. 2013). To ensure assay sensitivity, doxorubicin was used as a positive control, while the negative control (DMSO-treated cells) was employed to confirm baseline cell behavior without treatment effects. Cell viability was determined by comparing the measured absorbance to that of the negative control, which was set at 100% cell viability. The dose-response curves were generated by treating cells with a concentration range of 10 to 1000 µM of each compound, allowing assessment of their cytotoxic or inhibitory effects across a broad spectrum.

Acknowledgements

The authors express their gratitude to the Deanship of Scientific Research at the University of Jordan for their generous funding. Additionally, they appreciate the support of the Scientific Research Department at Zarqa University for providing the Biovia 2022 license.

Additional information

Conflict of interest

The authors have declared that no competing interests exist.

Ethical statements

The authors declared that no clinical trials were used in the present study.

The authors declared that no experiments on humans or human tissues were performed for the present study.

The authors declared that no informed consent was obtained from the humans, donors or donors' representatives participating in the study.

The authors declared that no experiments on animals were performed for the present study.

The authors declared that no commercially available immortalised human and animal cell lines were used in the present study.

Funding

This work was supported by Deanship of Scientific Research at the University of Jordan.

Author contributions

Almeqdad Y. Habashneh design, synthesis the desired compounds, securing funding, conducting investigations, project administration, writing and revising the manuscript. Prof. Mahmoud A. Al-Sha'er conducts molecular docking and aims to understand the mechanism of action, as well as In-Silico ADMET analysis. Dr. Mervat S. Sammor is responsible for writing and analyzing data such as NMR and HRMS. Prof. Sanaa K. Bardaweel conducts cell culture analysis on Caco2 and HCT116 cell lines and handles the analysis, including MTT methodology, validation, and software usage. All co-authors have made significant contributions to the manuscript and unanimously agree to its submission with no conflicts of interest. Mustafa M El- Abadelah (May rest in Peace) Proposed and design the desired compounds.

Author ORCIDs

Mervat S. Sammor https://orcid.org/0009-0008-9738-7681
Almeqdad Y. Habashneh https://orcid.org/0000-0002-4001-1367
Mahmoud A. Al-Sha'er https://orcid.org/0000-0001-9962-1971
Sanaa K. Bardaweel https://orcid.org/0000-0002-4823-0708
Mustafa M. El-Abadelah https://orcid.org/0000-0003-2663-3677

Data availability

While preparing this work, the author(s) used QuillBot and Grammarly to improve the grammar and check for spelling errors. After using this tool/service, the author(s) reviewed and edited the content as needed and take(s) full responsibility for the publication's content.

References

Al-Sha'er MA, Almazari IS, Taha MO (2017) Discovery of novel potent nuclear factor kappa-B inhibitors (IKK-β) via extensive ligand-based modeling and virtual screening. Journal of Molecular Recognition 30: e2604. https://doi.org/10.1002/jmr.2604 [PMID: 28008665]

Al-Sha'er MA, Basheer HA, Taha MO (2023) Discovery of new PKN2 inhibitory chemotypes *via* QSAR-guided selection of docking-based pharmacophores. Molecular Diversity 27: 443–462. https://doi.org/10.1007/s11030-022-10434-4

Al-Sha'er MA, Mansi I, Khanfar M, Abudayyh A (2016) Discovery of new heat shock protein 90 inhibitors using virtual co-crystallized pharmacophore generation. Journal of Enzyme Inhibition and Medicinal Chemistry 31: 64–77. https://doi.org/10.1080/14756366.2016.1218485

Aly MF, Grigg R (1988) X= Y-ZH systems as potential 1, 3-dipoles: Part 20. Decarboxylation of α-imino acids. Mechanism and applications to thioamide synthesis. Tetrahedron 44: 7271–7282. https://doi.org/10.1016/S0040-4020(01)86099-3

Bacher N, Tiefenthaler M, Sturm S, Stuppner H, Ausserlechner MJ, Kofler R, Konwalinka G (2006) Oxindole alkaloids from Uncaria tomentosa induce apoptosis in proliferating, G0/G1-arrested and bcl-2-expressing acute lymphoblastic leukemia cells. British journal of haematology 132: 615–622. https://doi.org/10.1111/j.1365-2141.2005.05907.x

Barakat A, Islam MS, Ali M, Al-Majid AM, Alshahrani S, Alamary AS, Yousuf S, Choudhary MI (2021) Regio- and Stereoselective Synthesis of a new Series of spirooxindole pyrrolidine grafted thiochromene scaffolds as potential anticancer agents. Symmetry 13: 1426. https://doi.org/10.3390/sym13081426

Barakat A, Islam MS, Ghawas HM, Al-Majid AM, El-Senduny FF, Badria FA, Elshaier YAMM, Ghabbour HA (2018) Substituted spirooxindole derivatives as potent anticancer agents through inhibition of phosphodiesterase 1. RSC advances 8: 14335–14346. https://doi.org/10.1039/C8RA02358A

Bardaweel SK, Abu-Dahab R, Almomani, NF (2013) An in vitro based investigation into the cytotoxic effects of D-amino acids. Acta Pharmaceutica 63: 467–478. https://doi.org/10.2478/acph-2013-0032

Bora D, Kaushal A, Shankaraiah N (2021) Anticancer potential of spiro compounds in medicinal chemistry: A pentennial expedition, European Journal of Medicinal Chemistry 215: 113263–113239. https://doi.org/10.1016/j.ejmech.2021.113263

Bubna AK (2015) Vorinostat-An Overview. Indian journal of dermatology 60: 419. https://doi.org/10.4103/0019-5154.160511

Cui CB, Kakeya H, Osada H (1996) Novel mammalian cell cycle inhibitors, spirotryprostatins A and B, produced by Aspergillus fumigatus, which inhibit mammalian cell cycle at G2/M phase. Tetrahedron 52: 12651–12666. https://doi.org/10.1016/0040-4020(96)00737-5

Cui CB, Kakeya H, Osada H (1996) Spirotryprostatin B, a novel mammalian cell cycle inhibitor produced by Aspergillus fumigatus. The Journal of Antibiotics 49: 832–835. https://doi.org/10.7164/antibiotics.49.832

Cunningham CE, MacAuley MJ, Vizeacoumar FS, Abuhussein O, Freywald A, Vizeacoumar FJ (2020) The CINs of polo-like kinase 1 in cancer. Cancers 1312: 2953. https://doi.org/10.3390/cancers12102953

Edmondon S, Danishefsky SJ, Sepp-Lorenzino L, Rosen N (1999) Total synthesis of spirotryprostatin A, leading to the discovery of some biologically promising analogues. Journal of the American Chemical Society 121: 2147–2155. https://doi.org/10.1021/ja983788i

Galliford CV, Scheidt KA (2007) Pyrrolidinyl-spirooxindole natural products as inspirations for the development of potential therapeutic agents. Angewandte Chemie International Edition 46: 8748–8758. https://doi.org/10.1002/anie.200701342

Garcı´a Gime´nez D, Garcı´a Prado E, Sa´enz Rodrı´guez T, Ferna´ndez Arche A, De la Puerta R (2010) Cytotoxic effect of the pentacyclic oxindole alkaloid mitraphylline isolated from Uncaria tomentosa bark on human ewing's sarcoma and breast cancer cell lines. Planta medica 76: 133–136. https://doi.org/10.1055/s-0029-1186048

Garcı´a Prado E, Garcı´a Gimenez MD, De la Puerta Va´zquez R, Espartero Sa´nchez JL, Sa´enz Rodriguez MT (2007) Antiproliferative effects of mitraphylline, a pentacyclic oxindole alkaloid of Uncaria tomentosa on human glioma and neuroblastoma cell lines. Phytomedicine 14: 280–284. https://doi.org/10.1016/j.phymed.2006.12.023

Garvey DR, Chhabra G, Ndiaye MA, Ahmad N (2021) Role of polo-like kinase 4 (PLK4) in epithelial cancers and recent progress in its small-molecule targeting for cancer management. Molecular cancer therapeutics 20: 632–640. https://doi.org/10.1158/1535-7163.MCT-20-0741

Girgis, AS, Zhao Y, Nkosi A, Ismail NS, Bekheit MS, Aboshouk DR, Aziz MN, Youssef MA, Panda SS (2025) The Therapeutic Potential of Spirooxindoles in Cancer: A Focus on p53–MDM2 Modulation. Pharmaceuticals 18: 274. https://doi.org/10.3390/ph18020274

Grigg R, Sridharan V (1993) In: Curran DP (Ed.) Advances incycloaddation, Jai Press, London 3: 161.

Habashneh AY, El-Abadelah MM, Abadleh MM, Voelter W (2012) Heterocycles [c]-fused onto indoloquinoxaline. synthesis of novel pyrano [2', 3': 4, 5] indolo [2, 3-b] quinoxalin-2-ones. Zeitschrift für Naturforschung B 67: 725–730. https://doi.org/10.5560/znb.2012-0131

Hamed R, Obeid RZ, Abu-Huwaij R (2023) Plant mediated-green synthesis of zinc oxide nanoparticles: An insight into biomedical applications. Nanotechnology Reviews 12(1): 20230112. https://doi.org/10.1515/ntrev-2023-0112

Jossang A, Jossang P, Hadi HA, Sevenet T, Bodo B (1991) Horsfiline, an oxindole alkaloid from horsfieldia superba. The Journal of Organic Chemistry 56: 6527–6530. https://doi.org/10.1021/jo00023a016

Kostova I (2005) Synthetic and natural coumarins as cytotoxic agents. Current Medicinal Chemistry-Anti-Cancer Agents 5: 29–46. https://doi.org/10.2174/1568011053352550

Lliaki S, Beyaert R, Afonina IS (2021) Polo-like kinase 1 (PLK1) signaling in cancer and beyond. Biochemical pharmacology 193: 114747. https://doi.org/10.1016/j.bcp.2021.114747

Panda SS, Girgis AS, Aziz MN, Bekheit MS (2023) Spirooxindole: a versatile biologically active heterocyclic scaffold. Molecules. 28: 618. https://doi.org/10.3390/molecules28020618

Pozdnev VF (1990) Improved method for synthesis of 7-amino-4-methylcoumarin. Chemistry of Heterocyclic Compounds 26: 264–265. https://doi.org/10.1007/BF00472539

Qiu, W, Plotnikova O, Feher M, Awrey DE, Chirgadze NY (2024) RCSB protein date bank. https://www.rcsb.org/structure/4JXF

Rehn S, Bergman J, Stensland B (2004) The three-component reaction between Isatin, α-Amino Acids, and Dipolarophiles. European Journal of Organic Chemistry 2004: 413–418. https://doi.org/10.1002/ejoc.200300621

Sampson PB, Liu Y, Forrest B, Cumming G, Li SW, Patel NK, Edwards L, Laufer R, Feher M, Ban FD, Awrey E, Mao G, Plotnikova O, Hodgson R, Beletskaya I, Mason JM, Luo X, Nadeem V, Wei X, Kiarash R, Madeira B, Huang P, Mak TW, Pan G, Pauls HW (2015) The discovery of polo-like kinase 4 inhibitors: identification of (1R, 2S)-2-(3-((E)-4-(((cis)-2, 6-dimethylmorpholino) methyl) styryl)-1H-indazol-6-yl)-5'-methoxyspiro[cyclopropane-1, 3'-indolin]-2'-one (CFI-400945) as a potent, orally active antitumor agent. Journal of medicinal chemistry 58: 147–169. https://doi.org/10.1021/jm5005336

Shahbaz M, Perween A, Momal U, Imran M, Ul Hassan MH, Naeem H, Mujtaba A, Hussain M, Alsagaby SA, Al Abdulmonem W (2025) Recent perspectives on anticancer potential of Coumarin against different Human malignancies: an updated review. Food Science & Nutrition 13: 4696. https://doi.org/10.1002/fsn3.4696

Suymka YeI, Red'kin RG, Shemchuk LA, Hlebova KV, Filimonova NI (2017) Synthesis and the antimicrobial activity of hexamethylene-N-maleinimidospiroindole-3,3'-pyrrolo[3,4-c]pyrrole derivative. Zhurnal Organichnoi ta Farmatsevtichnoi Khimii 15: 56–62. https://doi.org/10.24959/ophcj.17.929

Yeung SF, Zhou Y, Zou W, Chan WL, Ching YP (2022) TEC kinase stabilizes PLK4 to promote liver cancer metastasis. Cancer Letters 524: 70–81. https://doi.org/10.1016/j.canlet.2021.08.038

Yu B, Yu DO, Liu HM (2015) Spirooxindoles: Promising scaffolds for anticancer agents. European Journal of Medicinal Chemistry 97: 673–698. https://doi.org/10.1016/j.ejmech.2014.06.056

Zhanga L, Xu Z (2019) Coumarin-containing hybrids and their anticancer activities. European Journal of Medicinal Chemistry 181: 111587. https://doi.org/10.1016/j.ejmech.2019.111587

Zhang X, Wei C, Liang H, Han L (2021) Polo-like kinase 4's critical role in cancer development and strategies for Plk4-targeted therapy. Frontiers in Oncology 11: 587554. https://doi.org/10.3389/fonc.2021.587554

Zhao Q, Xiong SS, Chen C, Zhu HP, Xie X, Peng C, He G, Han B (2022) Discovery of spirooxindole-derived small-molecule compounds as novel HDAC/MDM2 dual inhibitors and investigation of their anticancer activity. Frontiers in Oncology 12: 972372. https://doi.org/10.3389/fonc.2022.972372

Zhao Y, Yu S, Sun W, Liu L, Lu J, McEachern D, Shargary S, Bernard D, Li X, Zhao T, Zou P, Sun D, Wang S (2013) A potent small-molecule inhibitor of the MDM2–p53 interaction (MI-888) achieved complete and durable tumor regression in mice. Journal of Medicinal Chemistry 56: 5553–5561. https://doi.org/10.1021/jm4005708

Zhou LM, Qu RY, Yang GF (2020) An overview of spirooxindole as a promising scaffold for novel drug discovery. Expert Opinion on Drug Discovery 15: 603–625. https://doi.org/10.1080/17460441.2020.1733526

Supplementary material 1

Full Charactarization of the desired spirooxindole compounds 4a-k

Authors: Mervat S. Sammor, Almeqdad Y. Habashneh, Mahmoud A. Al-Sha'er, Sanaa K. Bardaweel, Mustafa M. El- Abadelah

Data type: docx

Copyright notice: This dataset is made available under the Open Database License (http://opendatacommons.org/licenses/odbl/1.0). The Open Database License (ODbL) is a license agreement intended to allow users to freely share, modify, and use this Dataset while maintaining this same freedom for others, provided that the original source and author(s) are credited.

Link: https://doi.org/10.3897/pharmacia.72.e149240.suppl1